Gamma-ray and X-ray Shock Emission from Spider Binaries

C Venter[1], Z Wadiasingh[1,2], AK Harding[2], A Kopp[1,3]

[1]Centre for Space Research, North-West University, Potchefstroom, South Africa

[2]NASA Goddard Space Flight Center, MD, USA

[3]Institut für Theoretische Physik IV, Ruhr-Universität Bochum, D-44780 Bochum, Germany

Collaborators: MG Baring, M Böttcher, S Chandra

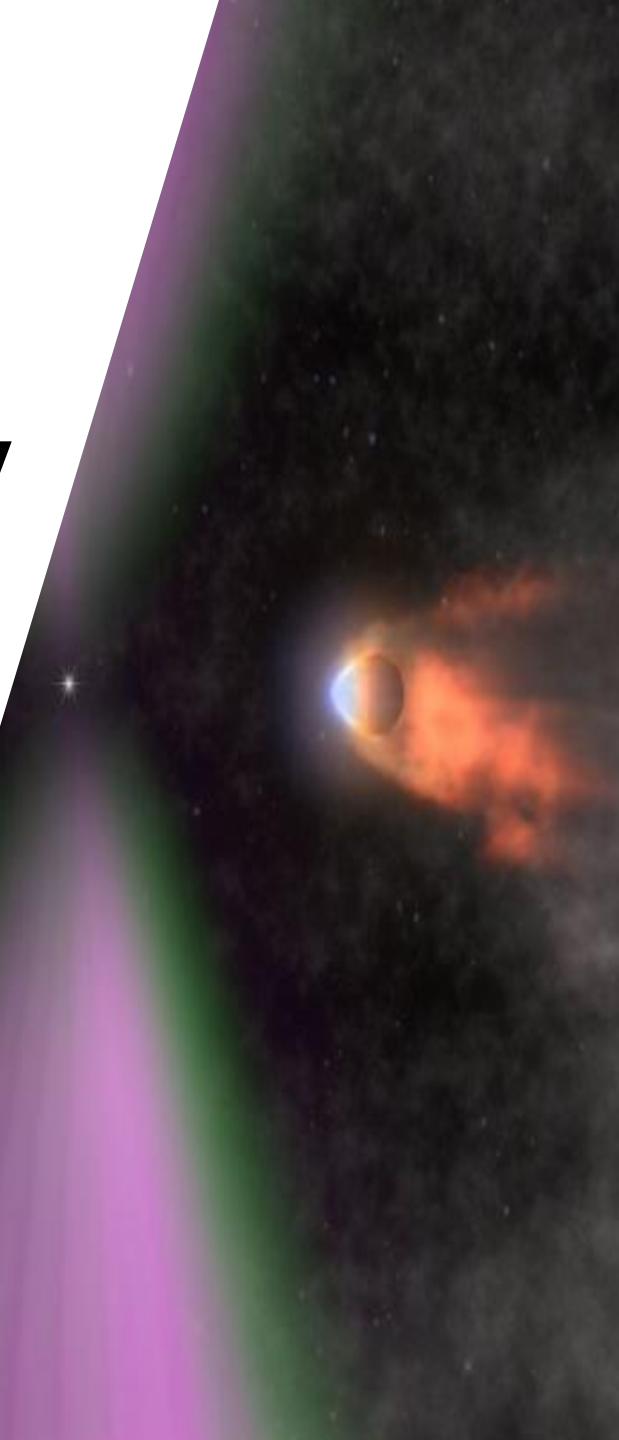

8th International *Fermi* Symposium

Baltimore, MD, USA, 14 – 19 October 2018

Spider Binaries

- Black widow (BW) & Redback (RB) spiders: devour male partners.
- Similar behaviour among pulsar binary systems.
- Low-mass star in close proximity to a millisecond pulsar: tight binaries P_b < 24 h.
- Intense pulsar wind heats tidally-locked companion and excites companion wind or even ablates it.
- Flares may occur on companion star: variable heating. Hot 'day side'.
- Interaction of pulsar and companion winds form intra-binary shock – site for particle acceleration.
- BWs: physically smaller and lower-mass companions (~0.01M_{sun}) than RBs (~0.1M_{sun}) .

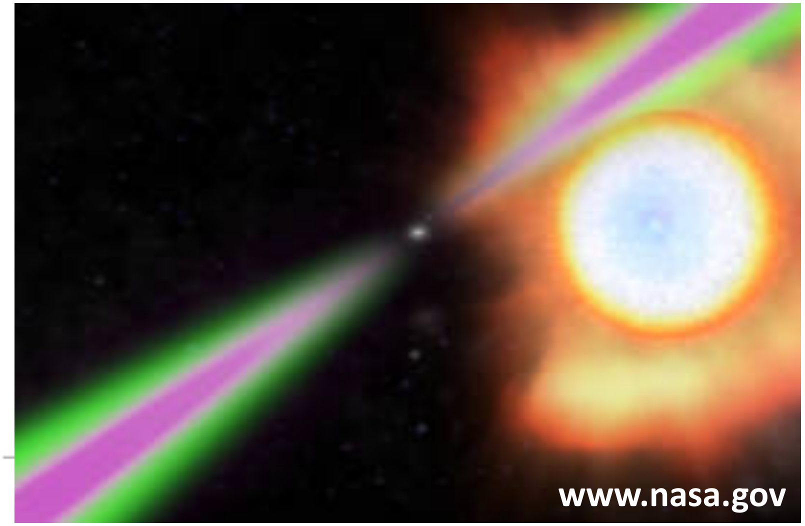

Fermi LAT Discoveries

- 96 millisecond pulsars discovered in unidentified *Fermi* LAT sources.
- ~22 black widows, ~9 redbacks (cf. P. Ray; >60 known in other bands).

Table 1
Measured and Derived Parameters of BW Pulsars

Name	P_{ms}	$\dot{P}_i$ (10^{-20})	L_{sd}[a] $(10^{34}$ erg s$^{-1})$	B_8[b]	d (kpc)	P_b (hr)	M_{comp} $(M_\odot)$	a_{11}	E_{cut} (TeV)	References
J0023+0923[c]	3.05	1.15	2.50	4.88	0.7	3.3	0.016	1.01	2.40	(1)
J0610–2100[c]	3.86	0.34	0.36	2.96	3.5	6.9	0.025	1.65	3.04	(2)
J1124–3653[c]	2.41	0.57	2.50	3.05	1.7	5.4	0.027	1.40	2.03	(1)
J1301+0833[c]	1.84	0.95	9.36	3.44	0.7	6.5	0.024	1.59	1.37	(3)
J1311–3430[c]	2.56	2.08	7.64	6.01	1.4	1.56	0.008	0.61	2.33	(4)
J1446–4701[c]	2.19	1.01	5.93	3.88	1.5	6.7	0.019	1.62	1.52	(5)
J1544+4937[c]	2.16	0.31	1.87	2.12	1.2	2.8	0.018	0.91	2.72	(6)
J1731–1847	2.34	2.47	11.9	6.26	2.5	7.5	0.04	1.75	1.23	(7)
J1745+1017[c]	2.65	0.23	0.75	2.02	1.36	17.5	0.016	3.07	1.86	(8)
J1810+1744[c]	1.66	0.45	6.08	2.26	2	3.6	0.044	1.07	1.86	(1)
J1959+2048[c]	1.61	0.72	10.6	2.80	1.53	9.2	0.021	2.00	1.19	(9)
J2047+1053[c]	4.29	2.00	1.56	7.63	2	3	0.035	0.95	2.78	(3)
J2051–0827[c]	4.51	1.23	0.83	6.14	1	2.4	0.027	0.82	3.51	(2)
J2214+3000[c]	3.12	1.46	2.96	5.57	1.32	10	0.014	2.11	1.59	(10), (11)
J2234+0944[c]	3.63	1.94	2.50	6.91	1	10	0.015	2.11	1.66	(3), (5)
J2241–5236[c]	2.19	0.67	3.90	3.15	0.5	3.4	0.012	1.03	2.12	(12)
J2256–1024[c]	2.29	1.58	8.11	4.96	0.6	5.1	0.034	1.35	1.54	(1)

Table 2
Measured and Derived Parameters of RB Pulsars

Name	P_{ms}	$\dot{P}_i$ (10^{-20})	L_{sd}[a] $(10^{34}$ erg s$^{-1})$	B_8[b]	d (kpc)	P_b (hr)	M_{comp} $(M_\odot)$	a_{11}	E_{cut} (TeV)	References
J1023+0038	1.69	1.20	15.4	3.72	0.6	4.8	0.2	1.33	1.33	(1)
J1628-3205	3.21	1.13	2.11	4.96	1.2	5	0.16	1.36	2.15	(2)
J1723-2837	1.86	0.75	7.18	3.08	0.75	14.8	0.4	2.90	1.09	(3), (4)
J1816+4510[c]	3.19	4.03	7.64	9.34	2.4	8.7	0.16	1.97	1.30	(5)
J2129-0429	7.61	43.54	6.08	47.4	0.9	15.2	0.37	2.94	1.12	(6)
J2215+5135[c]	2.61	2.79	9.67	7.03	3	4.2	0.22	1.22	1.55	(6)
J2339-0533[c]	2.88	1.39	3.59	5.21	0.4	4.6	0.26	1.30	1.93	(7), (8)

cf. Venter et al. (2015)

Radio Properties

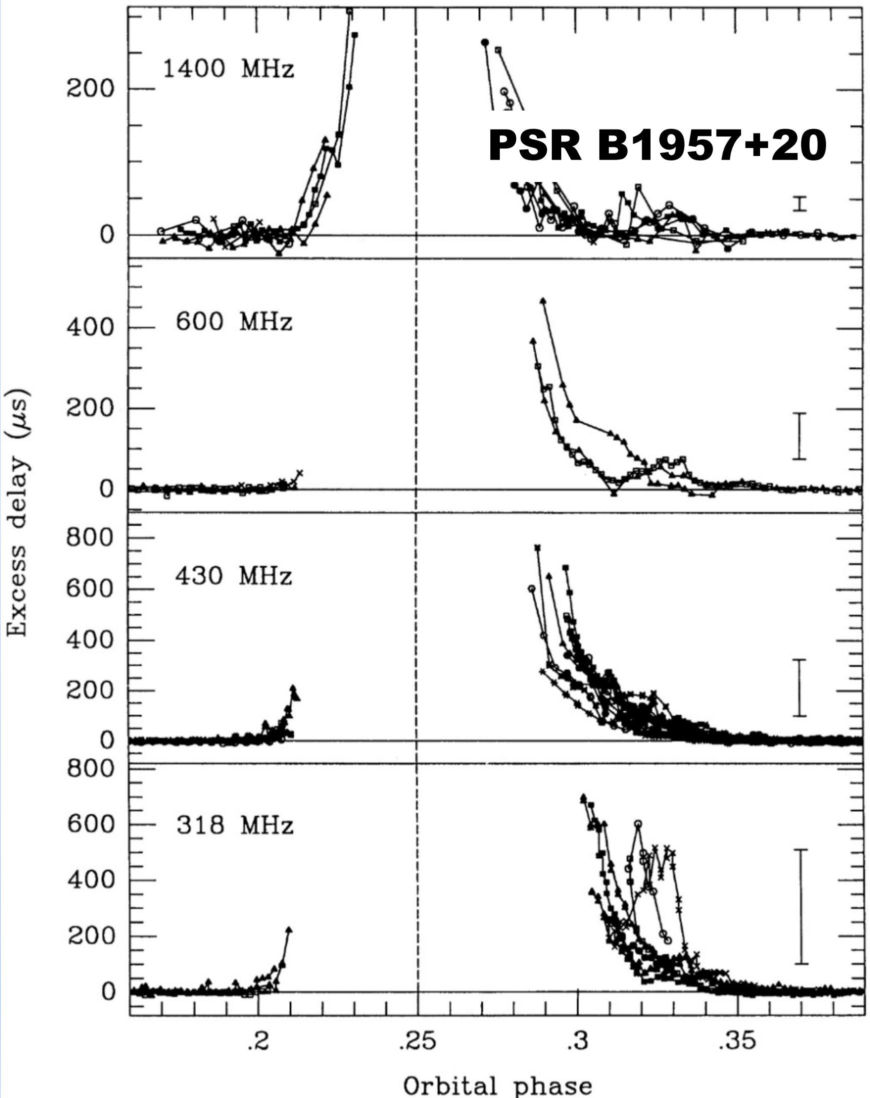

- **Many spider binaries exhibit frequency-dependent radio eclipses.**
- **Shrouding of MSP radio emission.**
- **Phase of eclipse discriminates shock orientation.**
- **Asymmetry of eclipse decreases with frequency: higher frequency observations probe denser regions closer to the shock.**

Ryba & Taylor (1991)

Optical Properties

- Photometry plus model of anisotropic heating: constrain system inclination.
- Heating: Variable, skewed shock or wind chanelling (Cho et al. 2018).
- Spectroscopic radial velocity studies: constrain mass ratio.
- Typical T_{comp} ~ 10^4 K; flaring states.
- Radio + optical mass functions: constrain pulsar mass.

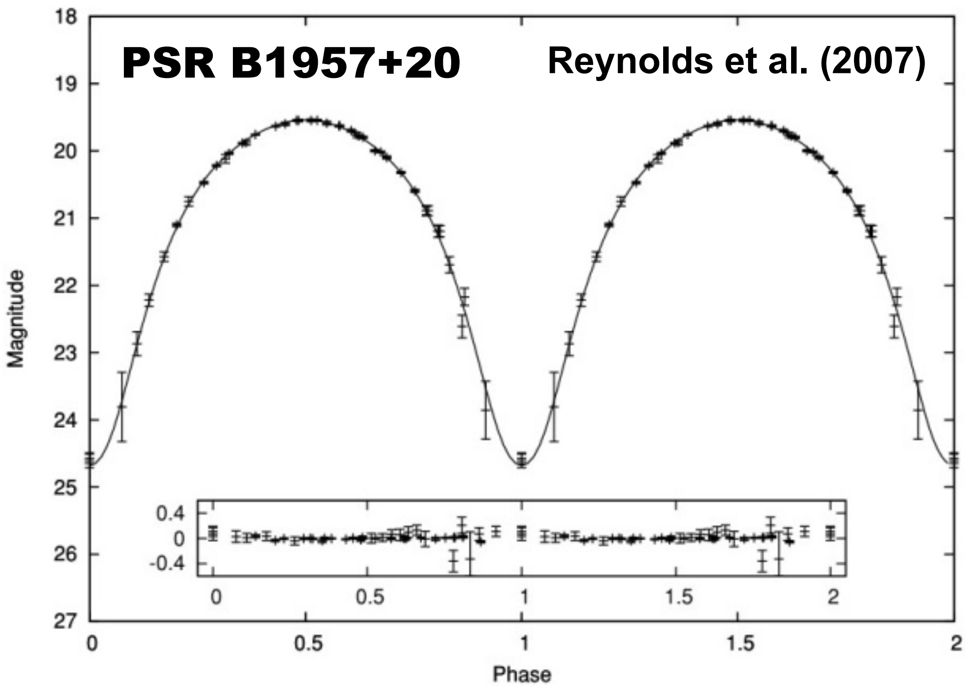

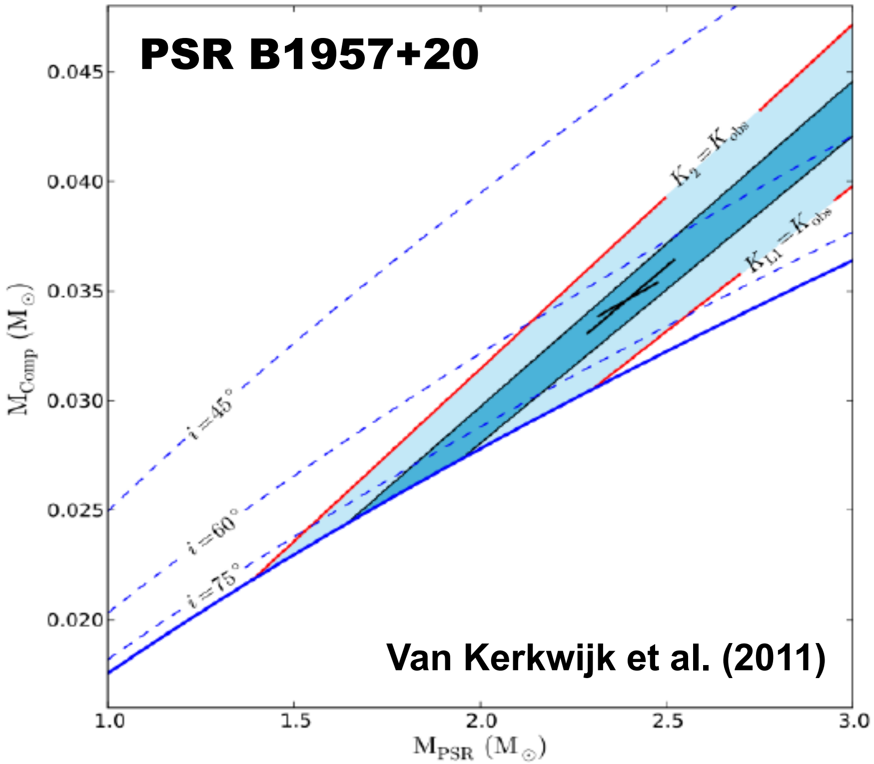

Credit: Z Wadiasingh

X-ray Properties

- Double-peaked emission: Doppler-boosted synchrotron emission from the intra-binary shock.
- Hard power laws: emission due to hard underlying electron spectrum.
- Spectra extending up to 80 keV: constraints on $B_{sh} \sim 1$ G.

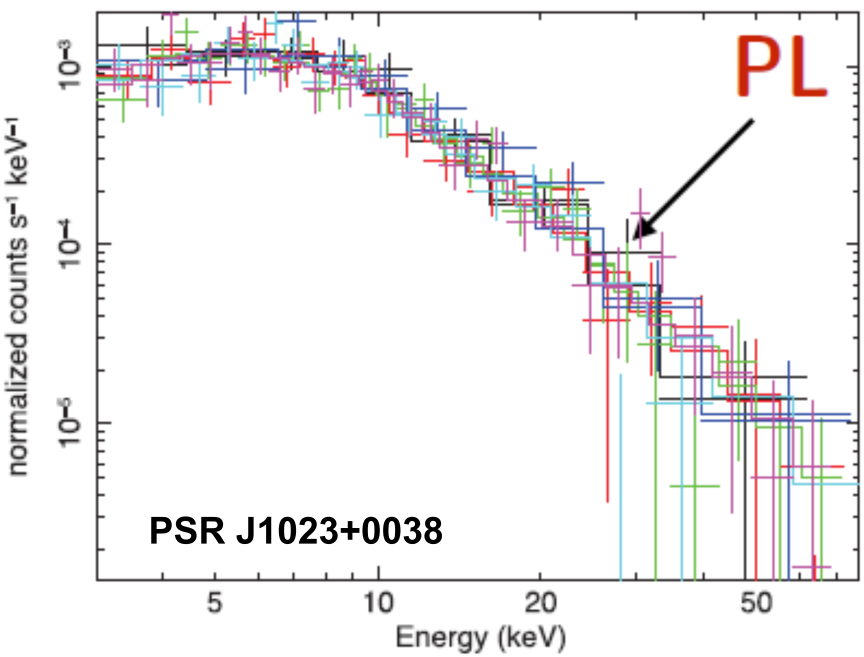

Tendulkar et al. (2014)

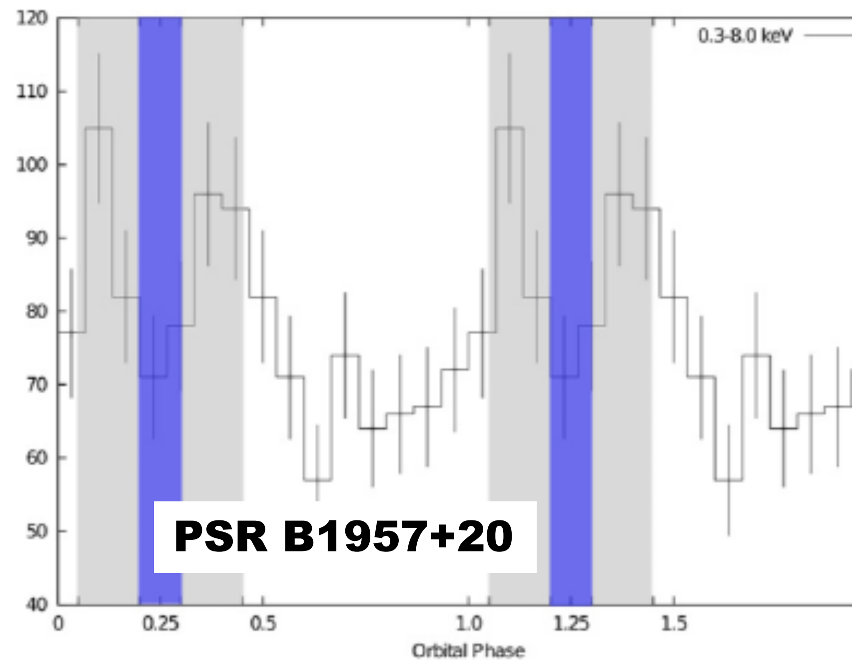

Huang et al. (2012)

cf. Wadiasingh et al. (2017)

Geometric X-ray LC Fitting

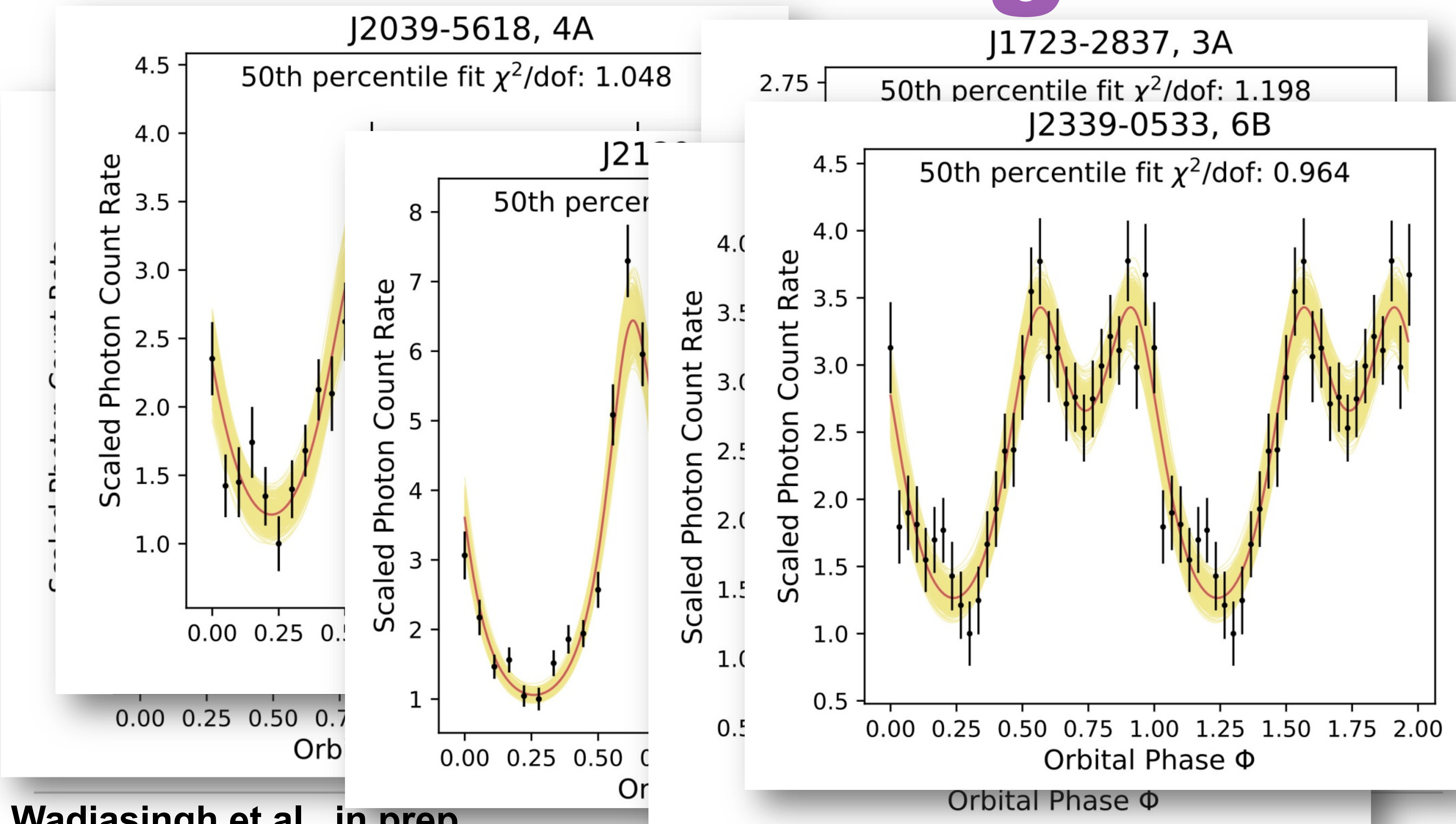

Wadiasingh et al., in prep.

γ-ray Properties

- Phase-aligned γ-ray and radio pulses from pulsar.
- No orbital modulation in GeV band.
- Upper limits in VHE band (MAGIC).

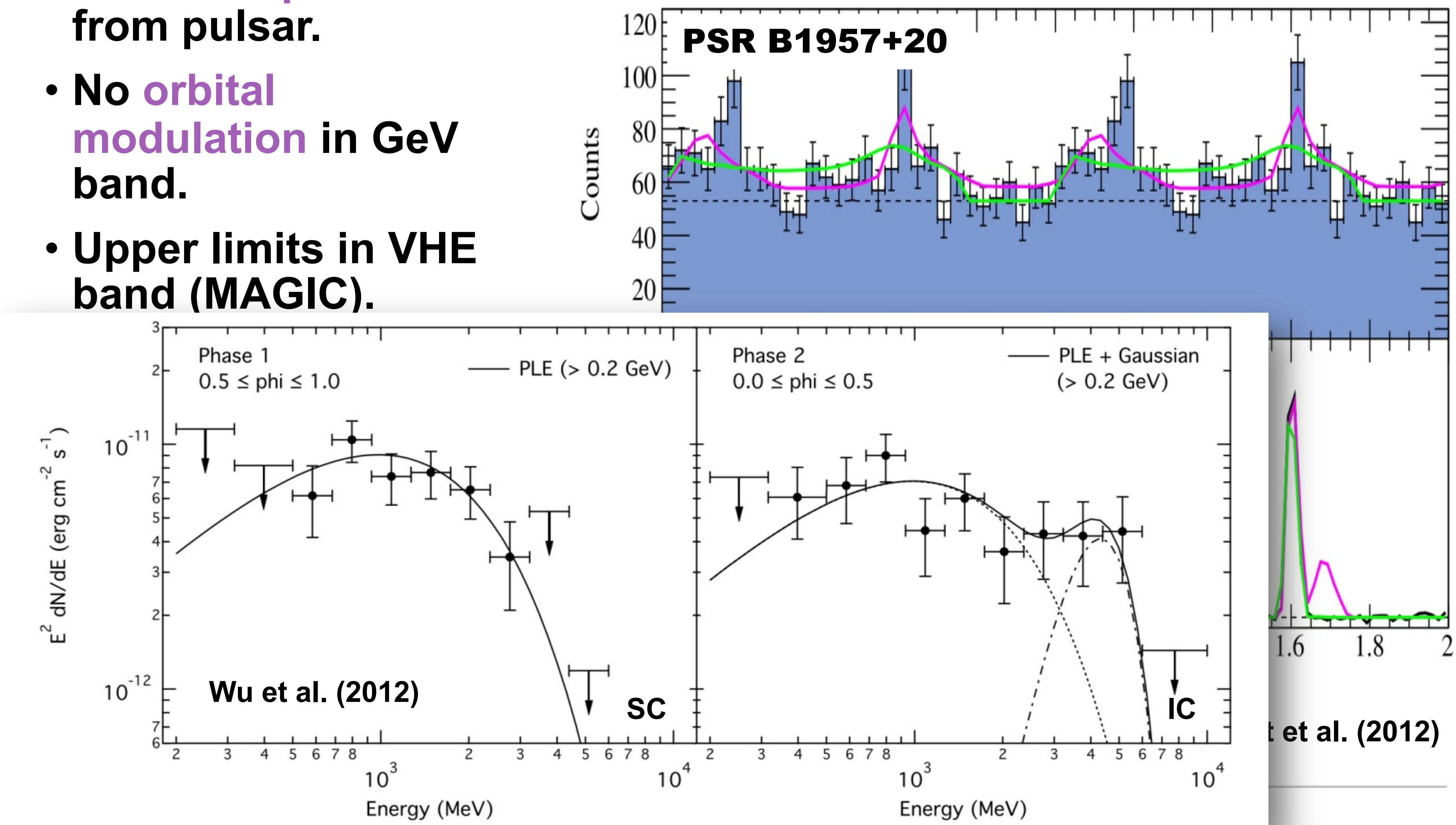

Intra-binary Shock

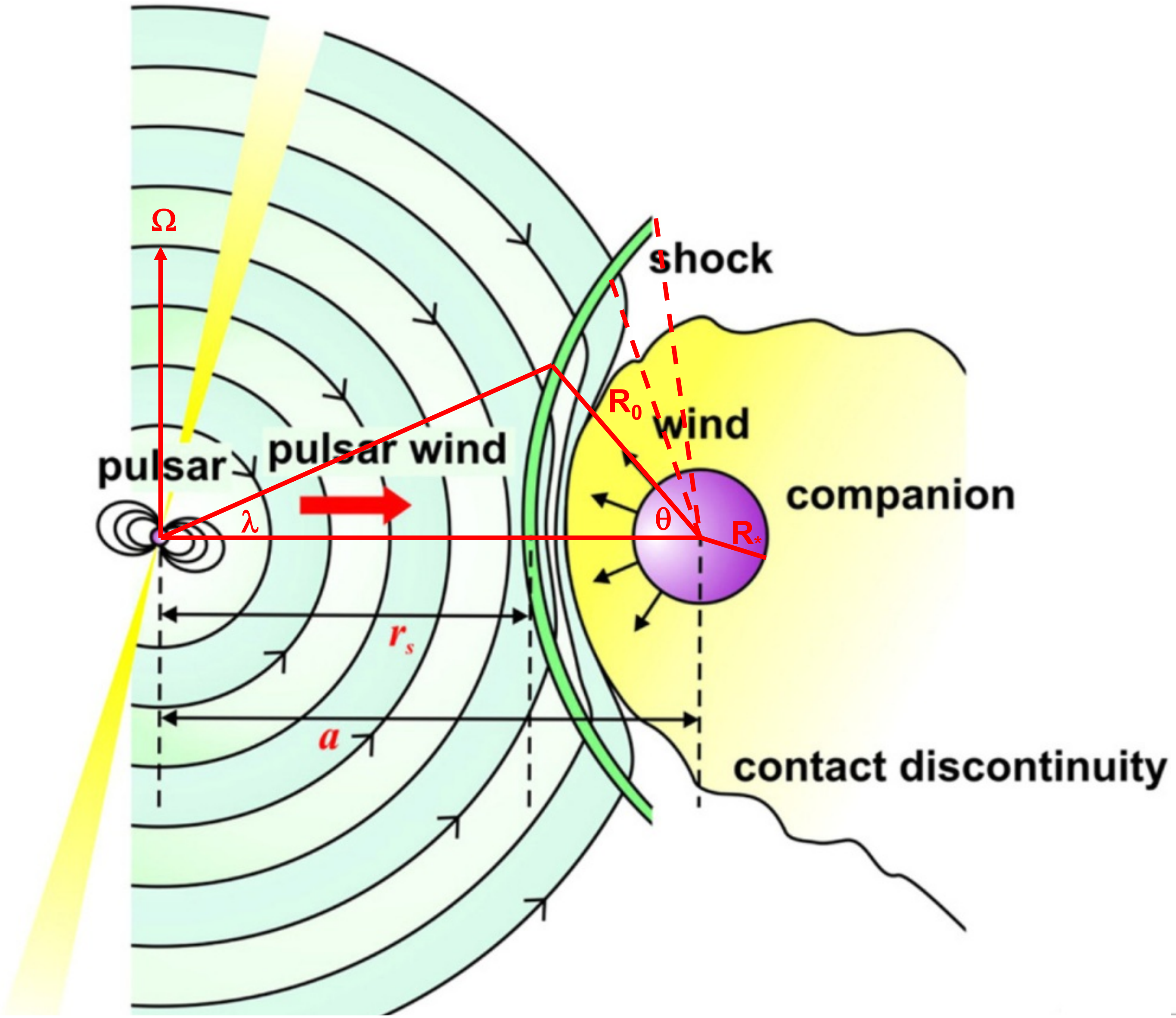

Venter et al. (2015); Harding & Gaisser (1990); Arons & Tavani (1993)

$\alpha = 15°$

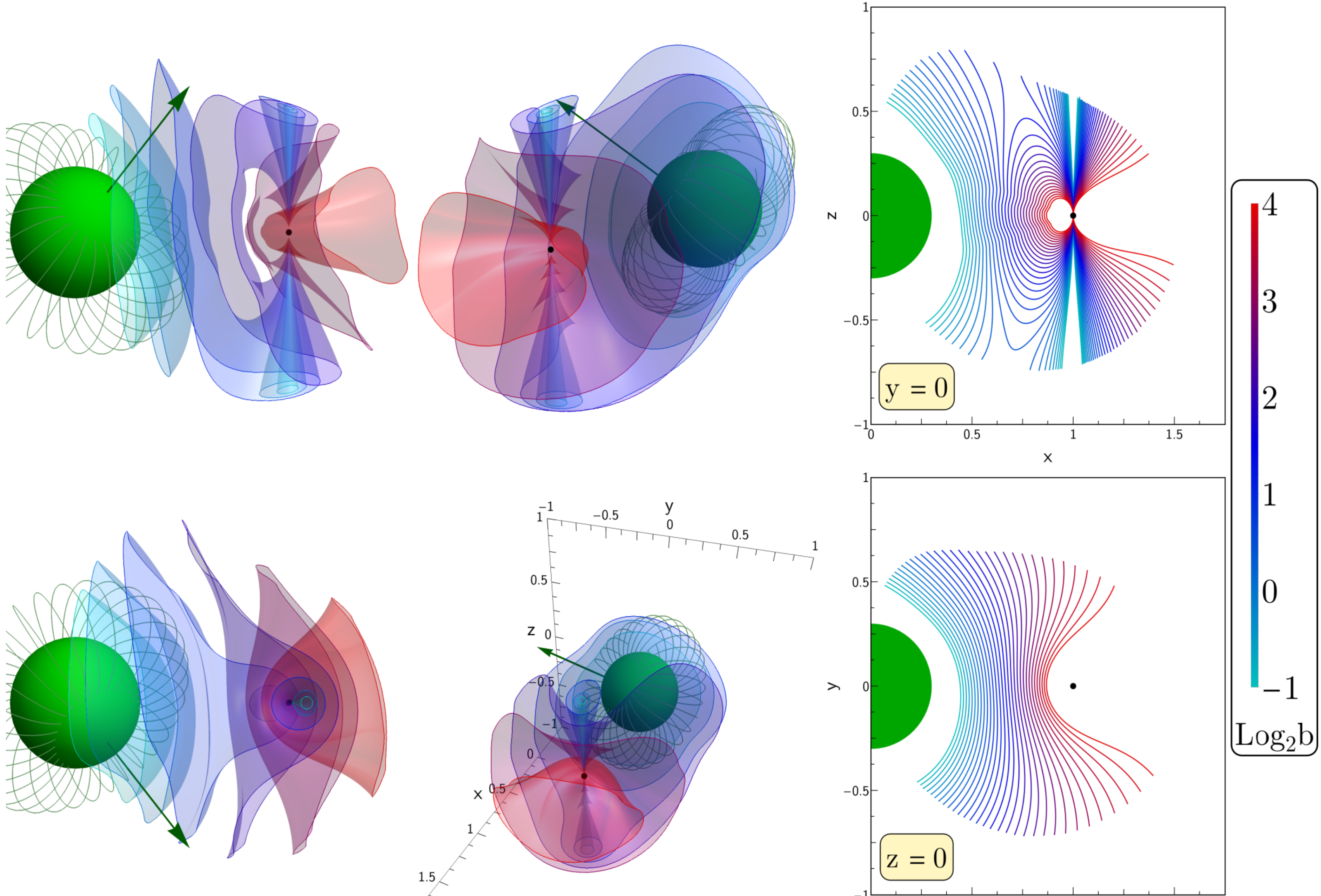

Wadiasingh et al., submitted; Tchekhovskoy et al. (2016)

Model Assumptions

1. Spherical polar cap shape for shock surrounding companion.
2. Azimuthal symmetry about line joining pulsar and companion $(d/d\phi = 0)$.
3. Steady-state $(d/dt = 0)$.
4. Isotropic black-body emission at temperature T from companion. Neglect SSC for now.
5. Approximate particle transport using timescales.
6. Isotropic steady-state particle spectrum in comoving frame.
7. Bulk flow: linear profile for $\beta\Gamma(\theta)$.

Injection Spectrum

Cut-off Energy:

$$E_{\mathrm{cut}} = eR_0 B_{\mathrm{sh}}$$

Solid Angle & Diffusion:

$$Q_{\mathrm{PSR}}(E_{\mathrm{e}}) = Q_0 E_{\mathrm{e}}^{-\Gamma} \exp\left(-\frac{E_{\mathrm{e}}}{E_{\mathrm{cut}}}\right)$$

$$Q_1 = \left(\frac{1}{4\pi}\int_0^{2\pi}\int_{\lambda_1}^{\lambda_2} \sin\lambda\, d\lambda\, d\phi\right) Q_{\mathrm{PSR}} = \frac{1}{2}\left(\cos\lambda_1 - \cos\lambda_2\right) Q_{\mathrm{PSR}}$$

$$Q_i = \frac{1}{t_{\mathrm{diff}}}\frac{dN_{\mathrm{e},i-1}}{dE_{\mathrm{e}}} + \frac{1}{2}\left(\cos\lambda_i - \cos\lambda_{i+1}\right) Q_{\mathrm{PSR}}, \quad i > 1$$

Normalisation - Current and Energetics:

$$\dot{N}_{\mathrm{GJ}} = \frac{B_{\mathrm{PSR}} 4\pi^2 R_{\mathrm{PSR}}^3}{2ceP^2} \qquad \dot{N}_{\mathrm{II}} = M_{\pm}\dot{N}_{\mathrm{GJ}}$$

$$\int_{E_{\min}}^{\infty} Q_{\mathrm{PSR}}\, dE_{\mathrm{e}} = (M_{\pm}+1)\dot{N}_{\mathrm{GJ}} \quad \int_{E_{\min}}^{\infty} E_{\mathrm{e}} Q_{\mathrm{PSR}}\, dE_{\mathrm{e}} = \eta_{\mathrm{p}}\dot{E}_{\mathrm{rot}}$$

Particle Transport

$$\frac{\partial N_e}{\partial t} = -\vec{V} \cdot \left(\vec{\nabla} N_e\right) + \kappa(E_e) \nabla^2 N_e + \frac{\partial}{\partial E_e}\left(\dot{E}_{e,tot} N_e\right) - \left(\vec{\nabla} \cdot \vec{V}\right) N_e + Q$$

$$N_e = Q\tau_{eff}$$

$$\tau_{eff}^{-1} = \tau_{ad}^{-1} + \tau_{diff}^{-1} + \tau_1^{-1} + \tau_2^{-1} + \tau_{rad}^{-1}$$

$$\tau_{ad} = \frac{3R_0}{c}\left[\frac{\partial \beta}{\partial \theta} + \beta \cot\theta\right]^{-1}$$

$$\tau_{rad} = \frac{E_e}{\dot{E}_{e,rad}}$$

$$\tau_1 = \frac{R_0}{c\beta \tan\theta}$$

$$\tau_2 = \frac{\tau_{ad}}{3}$$

$$\tau_{diff} = \frac{R_0^2}{2\kappa}$$

"Best Fit"

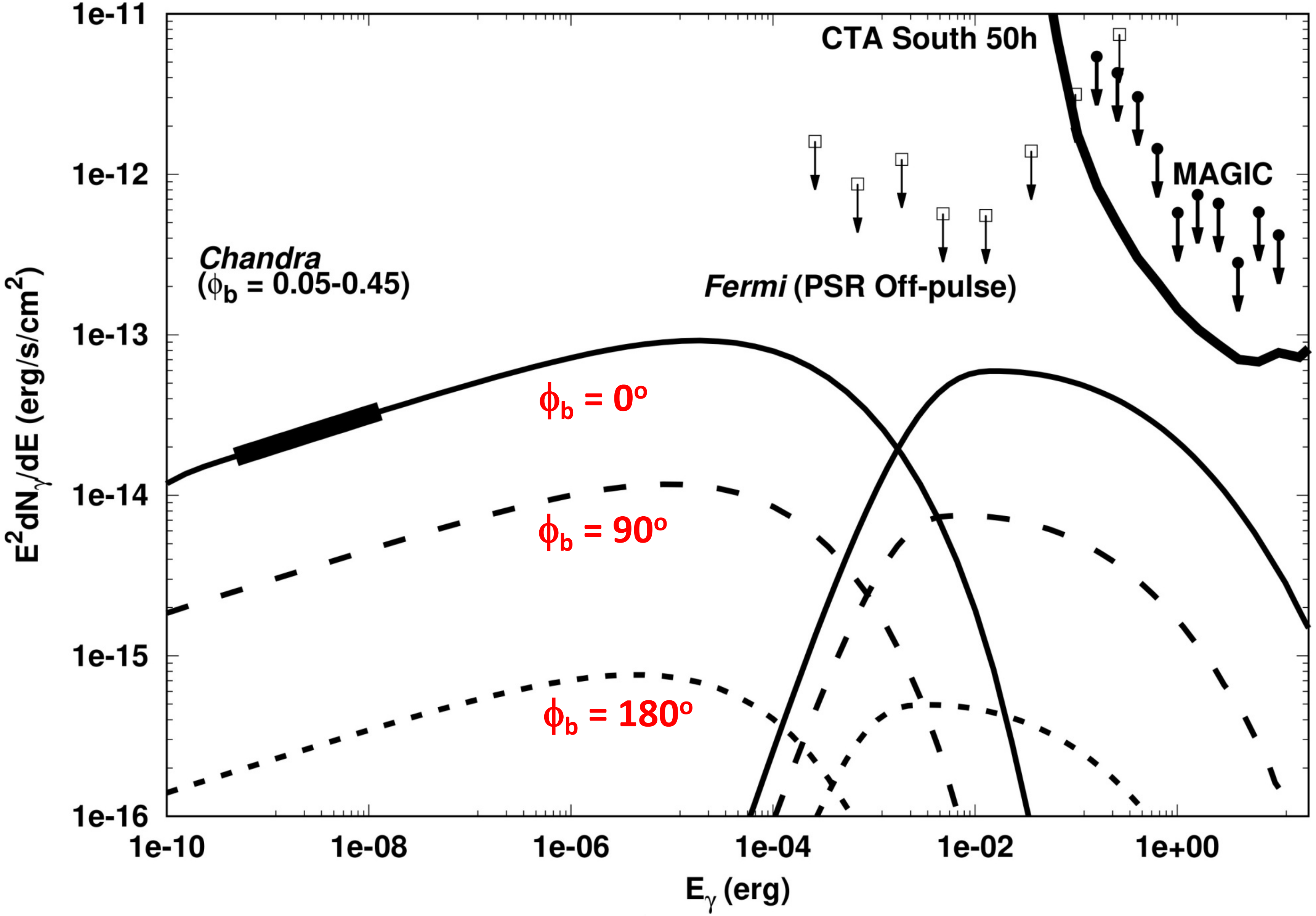
CTA South 50h
MAGIC
Chandra
(ϕb = 0.05-0.45)
Fermi (PSR Off-pulse)
ϕb = 0°
ϕb = 90°
ϕb = 180°
1e-11
1e-12
1e-13
1e-14
1e-15
1e-16
E²dNγ/dE (erg/s/cm²)
1e-10
1e-08
1e-06
1e-04
1e-02
1e+00
Eγ (erg)

Effect of Binary Separation

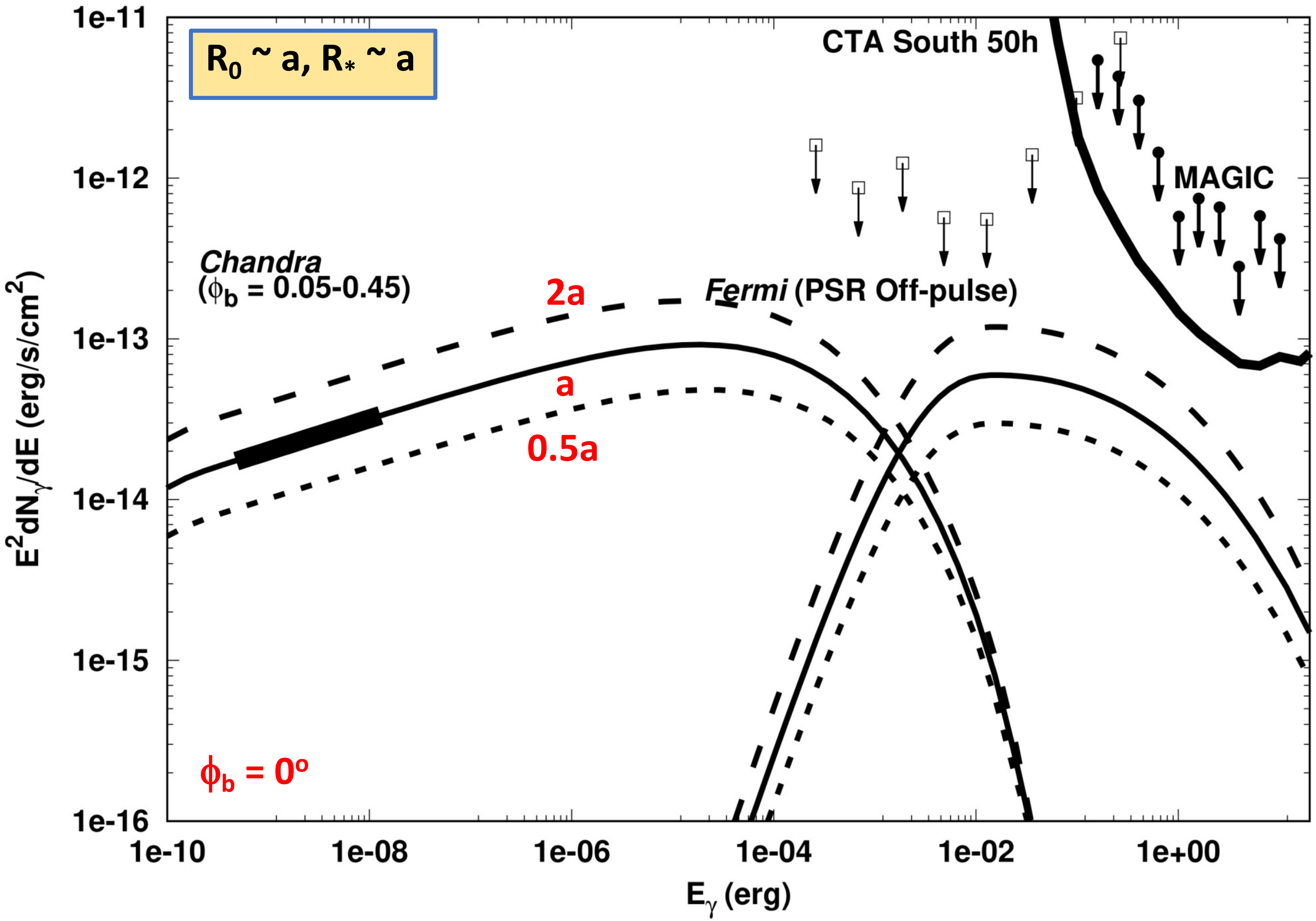

Effect of Stellar Radius

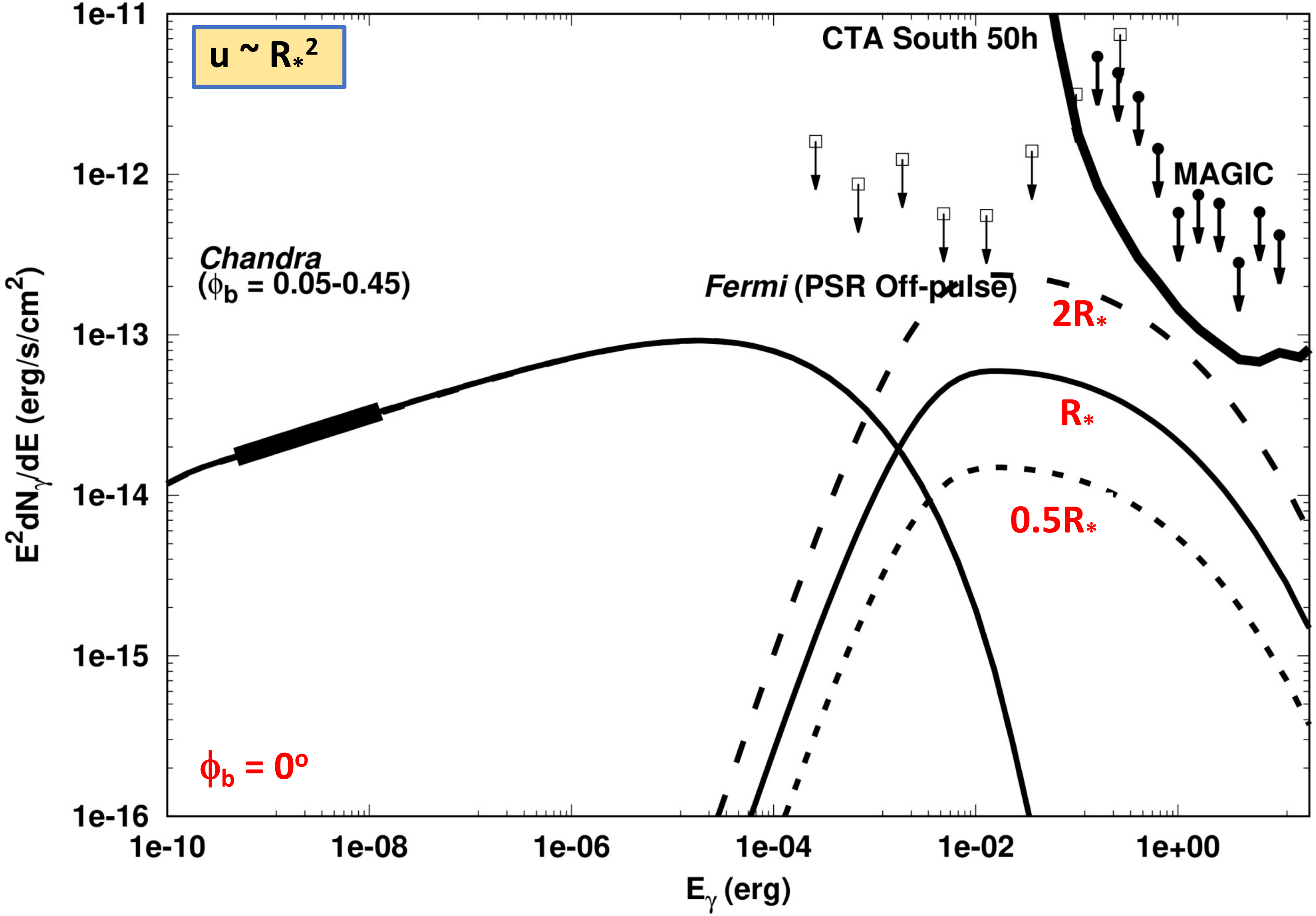

Effect of Shock *B*-field

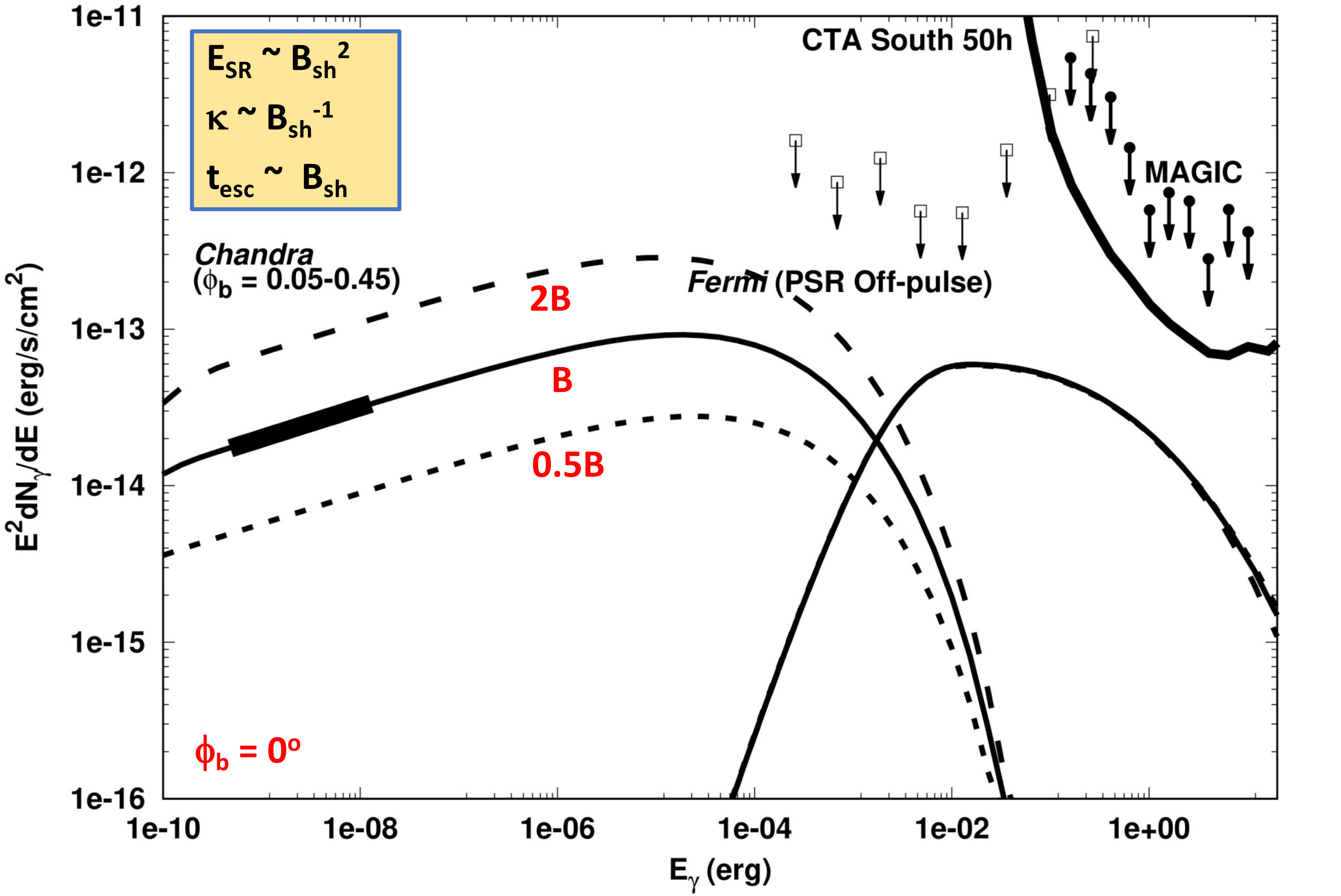

Effect of Injection Index

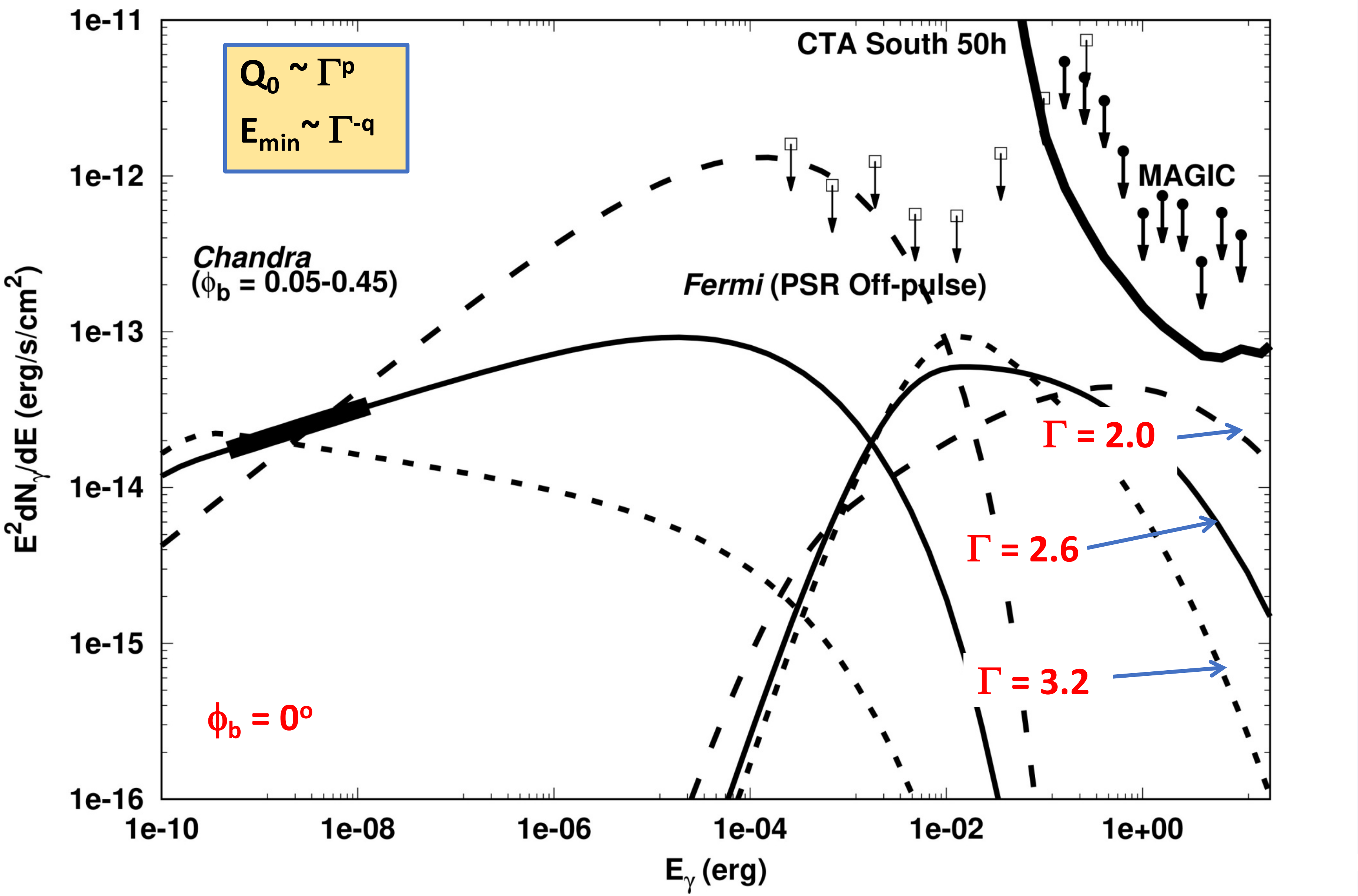

Rotation & Doppler Boosting

Tangent Velocity:

$$\boldsymbol{u}' \equiv \frac{dR_x}{d\theta}\hat{\boldsymbol{x}} + \frac{dR_y}{d\theta}\hat{\boldsymbol{y}} + \frac{dR_z}{d\theta}\hat{\boldsymbol{z}}, \qquad \hat{\boldsymbol{u}}' = \frac{\boldsymbol{u}'}{u'}$$

$$\hat{\boldsymbol{u}} = \Lambda_i \Lambda_{\Omega_b t_0} \hat{\boldsymbol{u}}'$$

$$\Lambda_i = \begin{pmatrix} \sin i & 0 & \cos i \\ 0 & 1 & 0 \\ -\cos i & 0 & \sin i \end{pmatrix}$$

$$\Lambda_{\Omega_b t} = \begin{pmatrix} \cos(\Omega_b t) & -\sin(\Omega_b t) & 0 \\ \sin(\Omega_b t) & \cos(\Omega_b t) & 0 \\ 0 & 0 & 1 \end{pmatrix}$$

Doppler Boosting Factor:

$$\delta = \frac{1}{\Gamma(1 - \beta \vec{n} \cdot \vec{u})}$$

Observed Energy Flux:

$$E = \delta E' \qquad \nu F_\nu = \delta^3 \nu' F'_\nu$$

SR LCs for different *i* & E_γ

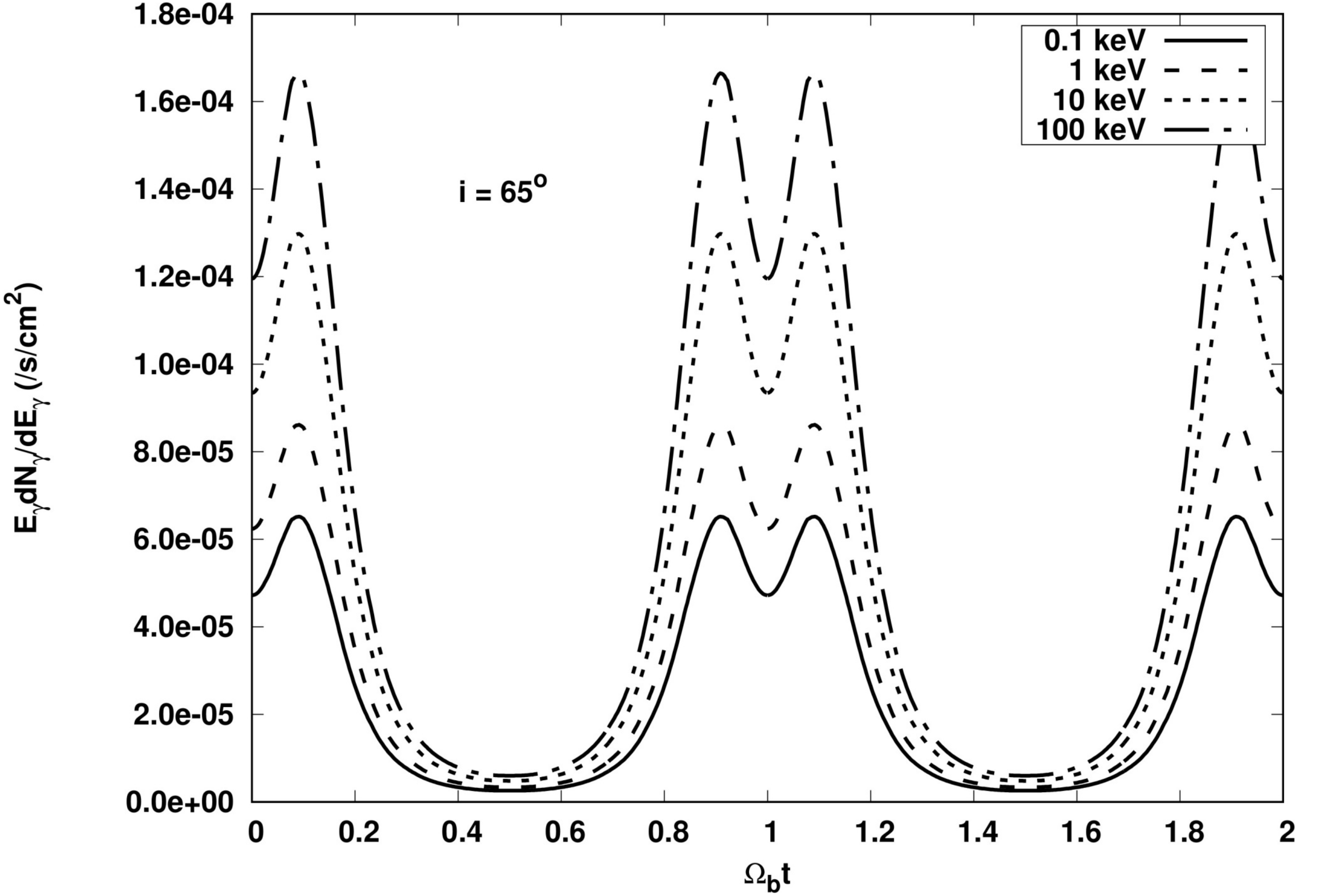

SR LCs for different i & E_γ

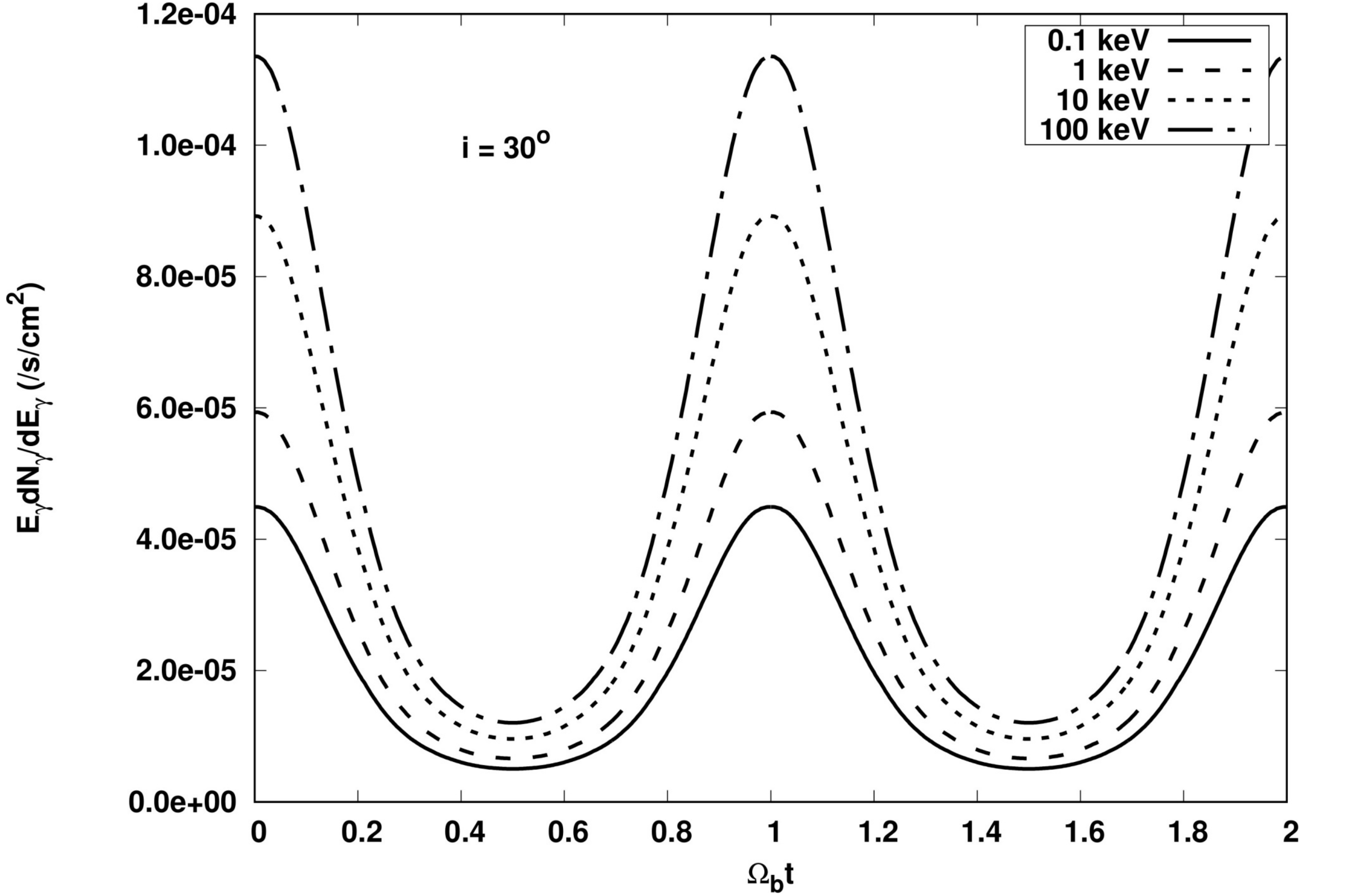

IC LCs for different *i* & E_γ

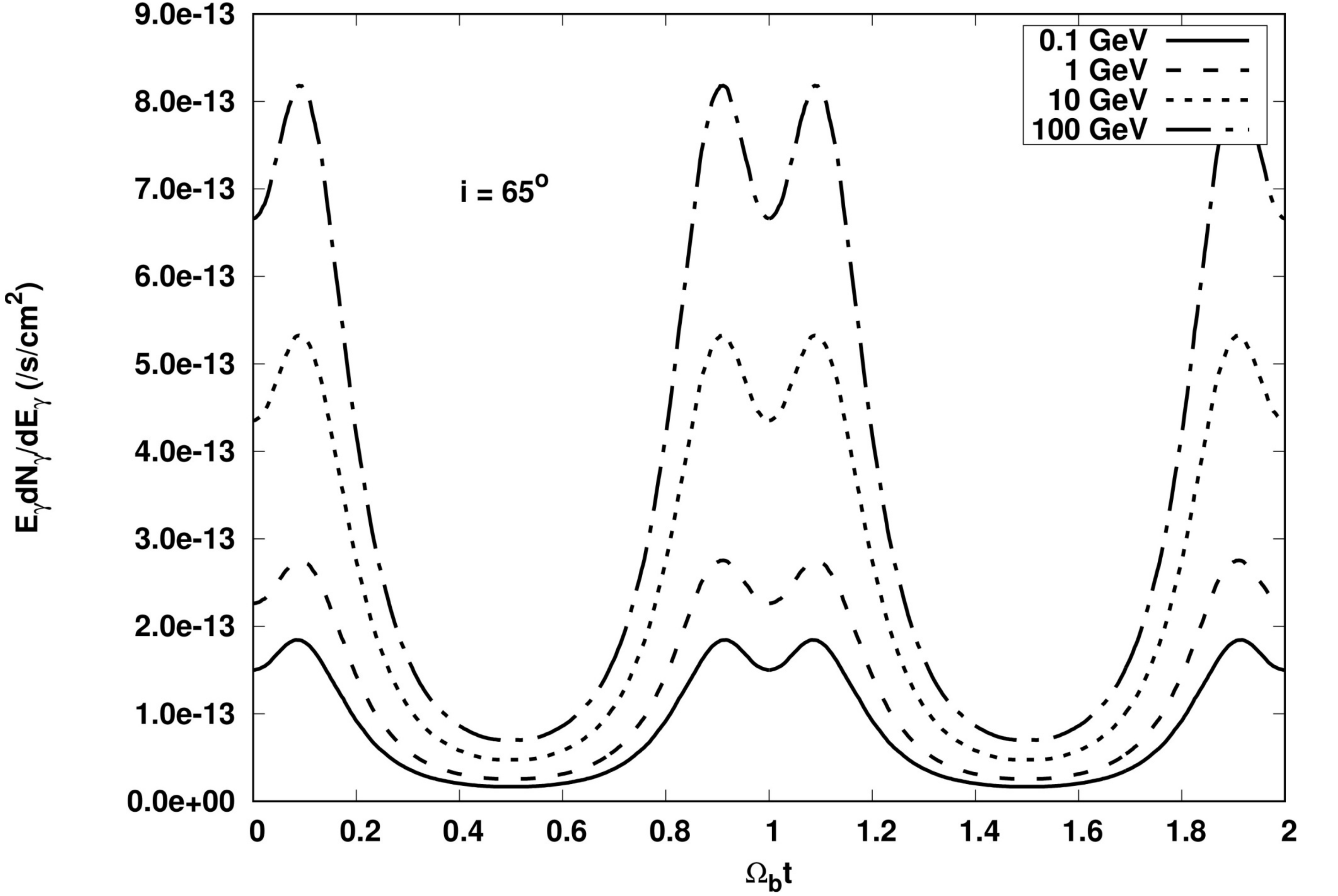

IC LCs for different i & E_γ

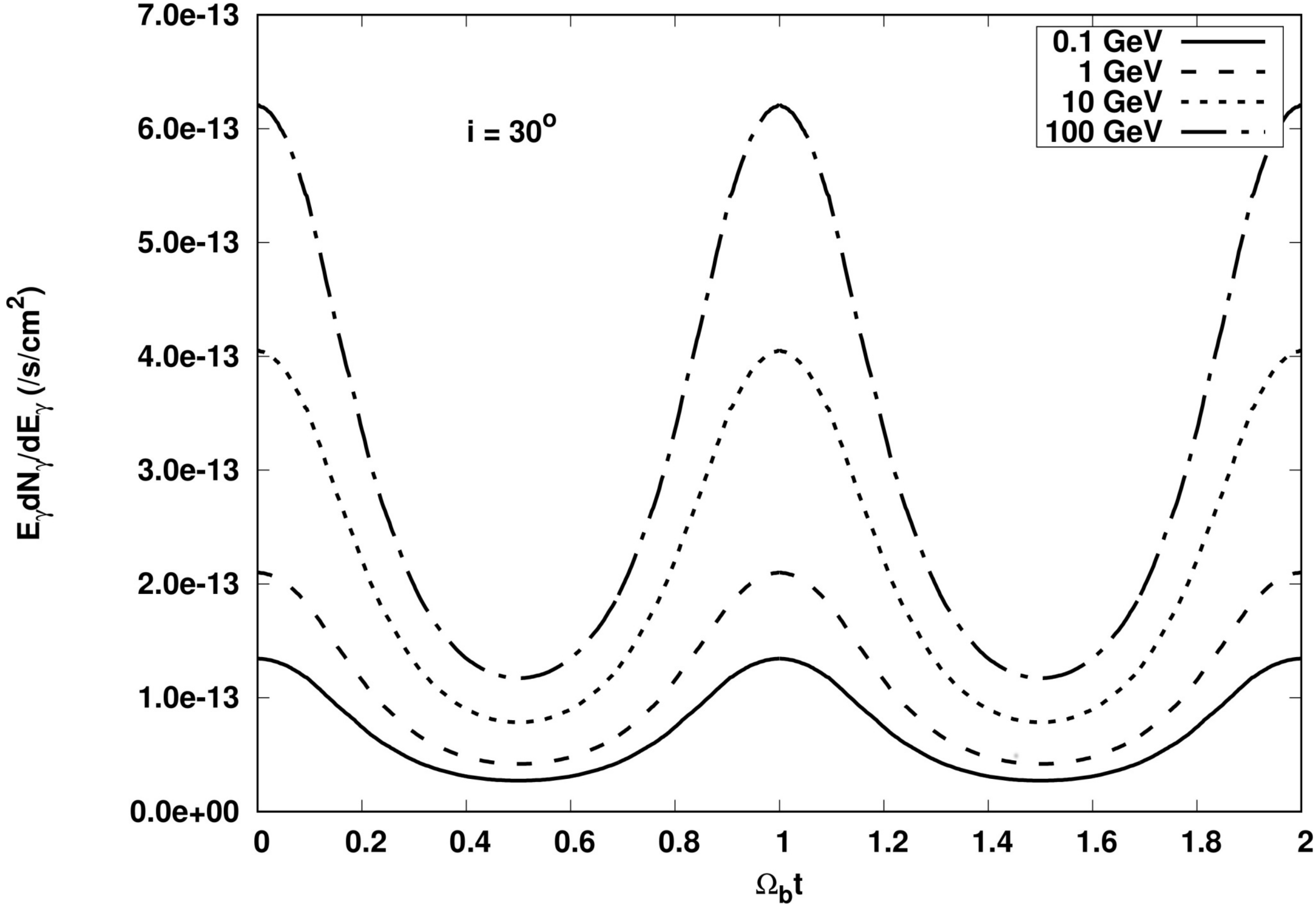

“Flare” – increase in Temperature

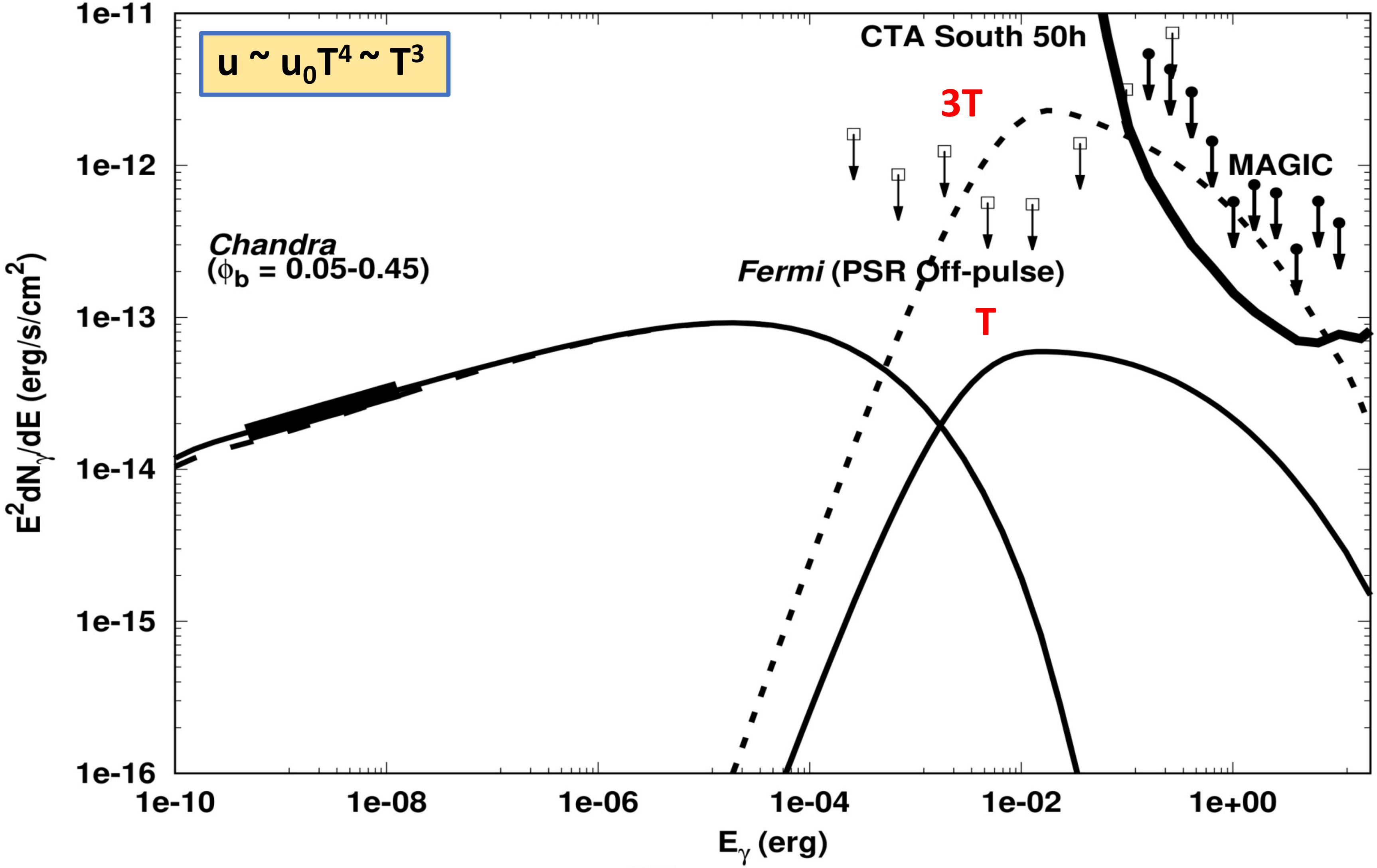

FUTURE: Other Components: Upstream IC; SSC

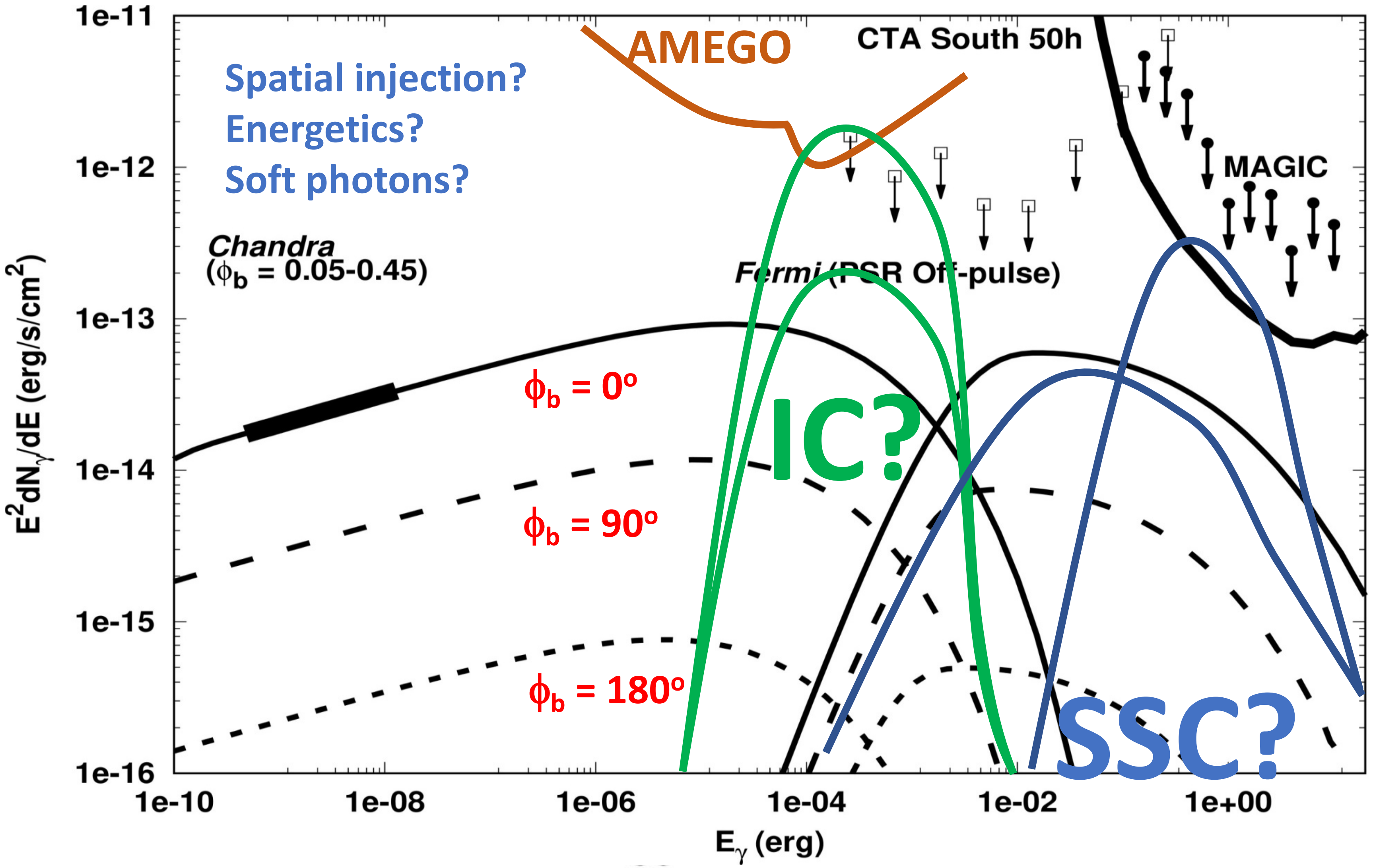

Conclusions

- **Modelling:**
  - ➢ **SR & IC flux from BWs: phase-resolved spectra and energy-dependent light curves.**
  - ➢ **Normalise using SR spectrum.**
  - ➢ **B1957+20 below *Fermi* & MAGIC upper limits.**
  - ➢ **Quite dependent on free parameters.**
- **Future refinements:**
  - ➢ **Apply model to more BWs and RBs.**
  - ➢ **Improved shock geometry.**
  - ➢ **Anisotropic IC, acceleration, shadowing.**
  - ➢ **SSC and upstream IC components.**

- **Promising targets for modulated SR / IC flux, especially energetic, flaring, nearby sources.**

Thanks!

This work is based on the research supported wholly / in part by the National Research Foundation of South Africa (Unique Grant Number 99072)

"O LORD our Lord, how majestic and glorious and excellent is Your Name in all the earth! You have displayed Your splendour above the heavens" (Psalm 8:1 AMP).